Trajectory Control of a Class of Articulated Aerial Robots

Marin Kobilarov
Laboratory for Computational Sensing and Robotics
Johns Hopkins University

***Abstract*—This paper studies trajectory control of aerial vehicles equipped with robotic manipulators. The proposed approach employs free-flying multi-body dynamics modeling and backstepping control to develop stabilizing control laws for a general class of underactuated aerial systems. A simulated hexrotor vehicle with a simple manipulator is employed to demonstrate the proposed techniques.**

I. Introduction and Related Work

Motivated by recent progress in aerial robotics this paper considers the trajectory control of articulated flying mechanisms capable of performing aerial manipulation tasks. Aerial systems equipped with manipulator arms have a number of potential applications, e.g. to pick-up and transport vital supplies or to reach difficult-to-access locations and perform emergency repairs. The ability to grasp and transport objects has recently been explored using small autonomous helicopters [1, 2] operating outdoors and using multiple coordinated quadrotors [3] to assemble indoor structures. A related problem is balancing an inverted rigid mass [4]. Equipping aerial vehicles with more complex multi-degree of freedom manipulators remains challenging due their limited payload capacity and inherent flight instability. Such issues are currently being explored in the context of the Mobile Manipulating Unmanned Aerial Vehicle (MM-UAV) project [5, 6, 7] and are also of interest in the recently established Airobots project [8] and (Aerial Robotics Cooperative Assembly System) ARCAS project [9]. A related problem studied previously deals with the dynamics of helicopters with external slung loads (e.g. [10]).

Motivated by these developments this work proposes a general nonlinear control strategy for aerial vehicles equipped with one or more articulated manipulators. A standard model simplification is to ignore rotational cross-coupling of lift forces and regard it as uncertainty during control [11, 12, 13]. Under such assumption our proposed methodology is applicable to any helicopter-type or any other multi-rotor-type vehicle. The paper develops a general trajectory control methodology with stability guarantees applicable to deterministic multi-body systems modeled as a tree-structure and controlled with lift and torque forces generated by propellers, and torques generated by the manipulator joint motors. While related to existing work on free-flying multi-body systems [14, 15, 16] the problem we consider poses a number of additional challenges arising from underactuation, gravity, and coupling between internal shape dynamics and overall system motion.

Standard methods for underactuated systems based on partial feedback linearization and *strong inertial coupling* [17] are not applicable, i.e. practically speaking there is no strong coupling between the uncontrolled accelerations in position space and the remaining degrees of freedom. On the other hand, it has been shown that controlling the position and the angle around the translation force input axis of a helicopter-like vehicle (modeled as single rigid body) is a choice that does not result in unstable *zero dynamics* [11]. Choosing these coordinates as outputs then renders the system differentially flat and feedback linearizable and appropriate virtual controls are found using dynamic decoupling [18] (or equivalently known as dynamic extension [19]). Such an approach is employed to control a number of quadrotor vehicles [20, 21, 22]. A number of methods have been recently proposed for controlling aerial vehicles using backstepping for better efficiency and disturbance rejection [13, 20, 23, 24, 25, 26, 27, 28]. A limitation of standard methods based on local coordinates is that the resulting controller is not globally valid and can result in singularities and unstable behavior, e.g. during inverted flight maneuvers. A method for tracking on manifolds [12] was proposed to overcome these limitations and achieve almost globally stable behavior. In addition, alternative methods for tracking on manifolds have been proposed [29, 30] that result in simpler control laws but rely on stronger assumptions such as boundedness on the maximum position error. Many of these methods have also been implemented successfully on a number of real vehicles.

The specific contributions of this work are to: 1) provide a general multi-body aerial vehicle modeling framework, 2) specify a coordinate change that enables tracking control with provable stability, 3) employ a coordinate-free formulation which avoids singularities, 4) give guidelines for implementing tasks that require simultaneous tracking of the system center-of-mass and the manipulator tip position. The proposed method currently does not account for uncertainty and control input bounds saturation which are critical for applications on real vehicles.

II. System Dynamics

The aerial vehicle is modeled as a mechanical system consisting of $n+1$ interconnected rigid bodies arranged in a tree structure. The configuration of body $\#i$ is denoted by

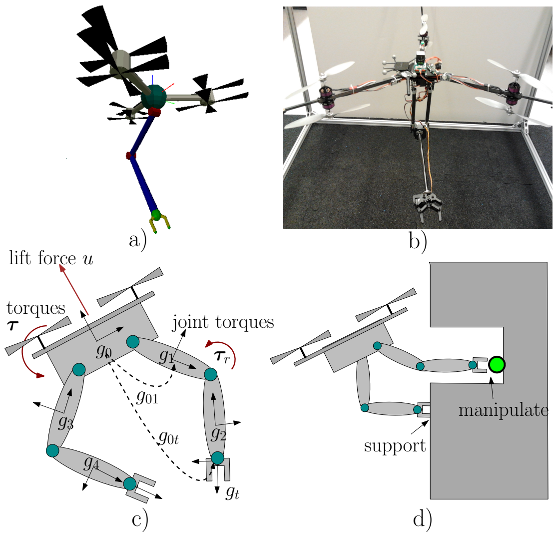

Fig. 1. a) simulated model of hex-rotor vehicle, b) a prototype robot with 3-dof manipulator in development, c) diagram of a typical multi-body aerial system, d) an imaginary scenario where aerial agility could play a key role.

$g_i \in SE(3)$, where

$$g_i = \begin{pmatrix} R_i & \boldsymbol{x}_i \\ 0 & 1 \end{pmatrix}, \quad g_i^{-1} = \begin{pmatrix} R_i^T & -R_i^T \boldsymbol{x}_i \\ 0 & 1 \end{pmatrix}.$$

where $\boldsymbol{x}_i \in \mathbb{R}^3$ denotes the position of its center of mass and and $R_i \in \mathrm{SO}(3)$ denotes its orientation. Its body-fixed angular and linear velocities are denoted by $\boldsymbol{\omega}_i \in \mathbb{R}^3$ and $\boldsymbol{v}_i \in \mathbb{R}^3$. The pose inertia tensor of each body is denoted by the diagonal matrix $\mathbb{I}_i$ defined by

$$\mathbb{I}_i = \begin{pmatrix} \mathbb{J}_i & 0 \\ 0 & m_i \boldsymbol{I}_3, \end{pmatrix}$$

where $\mathbb{J}_i$ is the rotational inertia tensor, m_i is the mass of body$\#i$, and $\boldsymbol{I}_3$ denotes the 3x3 identity matrix. Each body is subject to potential energy, e.g. due to gravity, defined by the function $V : SE(3) \to \mathbb{R}$. Assume that the base body #0 is subject to forces from propellers that result in body-fixed torque $\boldsymbol{\tau} \in \mathbb{R}^3$ and lift force $u > 0$ aligned with the constant body-fixed vertical axis $\boldsymbol{e} = (0, 0, 1) \in \mathbb{R}^3$.

The system has n joints described by parameters $\boldsymbol{r} \in M$, where $M \subset \mathbb{R}^n$ is the *shape space*. Following standard notation [31], denote the relative transformation between the base body#0 and body#i by $g_{0i} : M \to \mathrm{SE}(3)$, i.e.

$$g_i = g_0 g_{0i}(\boldsymbol{r}).$$

We assume that all joints are controlled using torque inputs denoted by $\boldsymbol{\tau}_r \in \mathbb{R}^m$.

A. Standard equations of motion in coordinates

The system dynamics can be written in standard form (e.g. [31]) according to

$$M(\boldsymbol{q})\ddot{\boldsymbol{q}} + C(\boldsymbol{q}, \dot{\boldsymbol{q}})\dot{\boldsymbol{q}} + g(\boldsymbol{q}) = B(\boldsymbol{q})\boldsymbol{u}, \tag{1}$$

where $\boldsymbol{q}$ are chosen coordinates describing e.g. the pose of the base body and all joints. While it is not difficult to express the dynamics in the form (1), for control purposes we will employ a slightly different formulation following previous methods for control on manifolds [12, 32] that avoid issues with rotational coordinates. In addition, we will employ a change of variables resulting in a simplified form for (1).

A typical choice of coordinates convenient for obtaining the dynamics is to employ the base body #0 as a reference. The Lagrangian of the system can then be written according to

$$L_0(\boldsymbol{q}_0, \boldsymbol{\xi}_0) = \frac{1}{2}\boldsymbol{\xi}_0^T M_0(\boldsymbol{r})\boldsymbol{\xi}_0 - \sum_{i=0}^{n} m_i \boldsymbol{a}_g^T \boldsymbol{x}_i, \tag{2}$$

where $\boldsymbol{q}_0 = (R_0, \boldsymbol{x}_0, \boldsymbol{r})$, $\boldsymbol{\xi}_0 = (\boldsymbol{\omega}_0, \boldsymbol{v}_0, \dot{\boldsymbol{r}})$, the positions $\boldsymbol{x}_1, \ldots, \boldsymbol{x}_n$ are regarded as functions of $\boldsymbol{q}_0$, and $\boldsymbol{a}_g$ denotes acceleration due to gravity. The mass matrix M_0 is defined by (e.g. see [31, 16])

$$M_0(\boldsymbol{r}) = \left[\begin{array}{c|c} \mathbb{I}_0 + \sum_{i=1}^{n} A_i^T \mathbb{I}_i A_i & \sum_{i=1}^{n} A_i^T \mathbb{I}_i J_i \\ \hline \sum_{i=1}^{n} J_i^T \mathbb{I}_i A_i & \sum_{i=1}^{n} J_i^T \mathbb{I}_i J_i \end{array}\right] \tag{3}$$

using the adjoint notation $A_i := \mathrm{Ad}_{g_{0i}^{-1}(\boldsymbol{r})}$, and Jacobian $J_i := g_{0i}^{-1}(\boldsymbol{r})\partial_{\boldsymbol{r}} g_{0i}(\boldsymbol{r})$.

B. Center-of-mass Coordinate Change

One can show that the equations of motion using coordinates $\boldsymbol{q}_0$ and the Lagrangian L_0 (2) result in coupling between all degrees of freedom (see §A). Despite this coupling, the position $\boldsymbol{x}_0$ can in practice be fully controlled only by orienting the base body in order to properly direct the main lift vector $\boldsymbol{e}u$. This is a non-trivial task since the reference body is subject to additional rotational and translational forces arising from the joint motions. We thus transform the system by change of coordinates that diagonalize the mass matrix with respect to the position. The rotation angle around the lift direction $\boldsymbol{e}$ and the transformed position coordinates thus become differentially flat outputs of the articulated multi-body system.

Let the matrices $\mathbb{J}, C, M_{\omega\dot{r}}, M_{v\dot{r}}, M_{\dot{r}\dot{r}}$ be defined by partitioning the mass matrix (3) according to

$$M_0(\boldsymbol{r}) = \left[\begin{array}{cc|c} \mathbb{J} & C^T & M_{\omega\dot{r}} \\ C & m\boldsymbol{I}_3 & M_{v\dot{r}} \\ \hline M_{\omega\dot{r}}^T & M_{v\dot{r}}^T & M_{\dot{r}\dot{r}} \end{array}\right], \tag{4}$$

where the total mass m is defined by $m = \sum_{i=0}^{n} m_i$. Our goal is to isolate the position dynamics which can be accomplished through diagonalization with respect to the $\boldsymbol{v}_0$-coordinates. This is equivalent to choosing new velocities $\boldsymbol{\xi} = (\boldsymbol{\omega}, \boldsymbol{v}, \boldsymbol{r})$ where

$$\boldsymbol{\omega} = \boldsymbol{\omega}_0, \tag{5}$$

$$\boldsymbol{v} = \boldsymbol{v}_0 + (M_{v\dot{r}}\dot{\boldsymbol{r}} + C\boldsymbol{\omega})/m, \tag{6}$$

which correspond to the new configuration $\boldsymbol{q} = (R, \boldsymbol{x}, \boldsymbol{r})$, where

$$R = R_0, \tag{7}$$

$$\boldsymbol{x} = \sum_{i=0}^{n} m_i \boldsymbol{x}_i. \tag{8}$$

It is clear that the new position $\boldsymbol{x}$ is simply the instantaneous center of mass of the whole system. Note that we have used the redundant notation $R \equiv R_0$ and $\boldsymbol{\omega} \equiv \boldsymbol{\omega}_0$ only to maintain consistency across all coordinates.

Proposition 1. *The equations of motion in coordinates $(\boldsymbol{q}, \boldsymbol{\xi})$ take the form:*

$$\dot{R} = R\boldsymbol{\omega}, \tag{9}$$

$$m\ddot{\boldsymbol{x}} = m\boldsymbol{a}_g + R\boldsymbol{e}u, \tag{10}$$

$$\begin{bmatrix} \boldsymbol{\omega} \\ \dot{\boldsymbol{r}} \end{bmatrix} = \overline{M}(\boldsymbol{r})^{-1} \begin{bmatrix} \boldsymbol{\mu} \\ \boldsymbol{\nu} \end{bmatrix}, \tag{11}$$

$$\begin{bmatrix} \dot{\boldsymbol{\mu}} \\ \dot{\boldsymbol{\nu}} \end{bmatrix} = \begin{bmatrix} \boldsymbol{\mu} \times \boldsymbol{\omega} \\ \frac{1}{2}\overline{\boldsymbol{\xi}}^T \partial \overline{M}(\boldsymbol{r}) \overline{\boldsymbol{\xi}} \end{bmatrix} + \begin{bmatrix} \boldsymbol{\tau} - C^T \boldsymbol{e}u/m \\ \boldsymbol{\tau}_r - M_{v\dot{r}}^T \boldsymbol{e}u/m \end{bmatrix}, \tag{12}$$

where $\overline{\boldsymbol{\xi}} = (\boldsymbol{\omega}, \dot{\boldsymbol{r}})$ and the mass matrix $\overline{M}(\boldsymbol{r})$ is

$$\overline{M} = \begin{bmatrix} \mathbb{J} - C^T C/m & M_{\omega\dot{r}} - C^T M_{v\dot{r}}/m \\ M_{\omega\dot{r}}^T - M_{v\dot{r}}^T C/m & M_{\dot{r}\dot{r}} - M_{v\dot{r}}^T M_{v\dot{r}}/m \end{bmatrix}. \tag{13}$$

Note that the main body and joint dynamics (12) were obtained in a form which leaves the body torques $\boldsymbol{\tau}$ and joint torques $\boldsymbol{\tau}_r$ decoupled. The rotational coupling is instead at the momentum level through the Legendre transform (11) which will be useful for the proposed passivity-based control design.

III. Trajectory Tracking

The tracking problem can be specified in a number of ways depending on the given task and available degrees of freedom. The manipulator end effector(s) frame is given by $g_t \in \mathrm{SE}(3)$ defined by

$$g_t = g_0 g_{0t}(\boldsymbol{r}), \tag{14}$$

where $g_{0t} : M \to \mathrm{SE}(3)$ is the local workspace transformation. One way to formulate the tracking task is using a subset or all of the end-effector desired pose g_{td}. For instance, if $\dim(M) = 2$ typically all six degrees of freedom of g_{td} can be satisfied subject to workspace constraints since there are four additional degrees of freedom that in principle can be satisfied using the aerial vehicle controls $(u, \boldsymbol{\tau}) \in \mathbb{R}^4$. Alternatively, it might be advantageous to specify a desired center of mass $\boldsymbol{x}_d$ and desired joint angles $\boldsymbol{r}_d$ and track them directly. In either case, tracking g_{td} can be accomplished by tracking corresponding $(\boldsymbol{x}_d, R_d, \boldsymbol{r}_d)$, where R_d should satisfy some additional conditions related to the system underactuation.

In particular, employing the notation of [12], in the context of helicopter backstepping, the desired rotation R_d is chosen to satisfy

$$R_d \boldsymbol{e} = \boldsymbol{\alpha}/u_d, \qquad u_d = \|\boldsymbol{\alpha}\|, \tag{15}$$

where

$$\boldsymbol{\alpha} = m\ddot{\boldsymbol{x}}_d - k_x(\boldsymbol{x} - \boldsymbol{x}_d) - k_v(\dot{\boldsymbol{x}} - \dot{\boldsymbol{x}}_d) - m\boldsymbol{a}_g.$$

This condition leaves one additional degree of freedom in R_d that can be specified by the user. Note that there could be multiple manipulators tracking their respective desired tip positions.

A. General Rotation Error

Errors in rotation are encoded using a *retraction map* $\vartheta : \mathbb{R}^3 \to \mathrm{SO}(3)$, i.e. a smooth map around the origin such that $\vartheta(\mathbf{0}) = I$, where I is the identity. In the following definitions the "hat" notation $\widehat{\cdot} : \mathbb{R}^3 \to \mathfrak{so}(3)$ defined by

$$\widehat{\omega} = \begin{bmatrix} 0 & -w^3 & w^3 \\ w^3 & 0 & -w^1 \\ -w^2 & w^1 & 0 \end{bmatrix}, \tag{16}$$

and its inverse $\check{\cdot} :\to \mathfrak{so}(3) \to \mathbb{R}^3$ are employed.

Definition III.1. The map $B_\vartheta : \mathrm{SO}(3) \to L(\mathbb{R}^3, \mathbb{R}^3)$ is such that, for a given $R \in \mathrm{SO}(3)$, the following holds

$$R = I + \widehat{\boldsymbol{\rho}} B_\vartheta(R^T),$$

where $\boldsymbol{\rho} = \vartheta^{-1}(R) \in \mathbb{R}^3$. There are three retraction map choices:

1) The *exponential map* $\vartheta = \exp$ and its inverse $\vartheta^{-1} = \log$ are defined by:

$$\exp(\boldsymbol{\rho}) = \begin{cases} \boldsymbol{I}_3, & \boldsymbol{\rho} = 0 \\ \boldsymbol{I}_3 + \frac{\sin\|\boldsymbol{\rho}\|}{\|\boldsymbol{\rho}\|}\widehat{\boldsymbol{\rho}} + \frac{1-\cos\|\boldsymbol{\rho}\|}{\|\boldsymbol{\rho}\|^2}\widehat{\boldsymbol{\rho}}^2, & \boldsymbol{\rho} \neq \mathbf{0} \end{cases} \tag{17}$$

$$\log(R) = \begin{cases} \mathbf{0}, & \theta = 0 \\ \frac{\theta}{2\sin\theta}\left(R - R^T\right)^{\vee}, & \theta \neq \mathbf{0} \end{cases} \tag{18}$$

$$B_{\exp}(R) = \begin{cases} \boldsymbol{I}_3, & \boldsymbol{\rho} = 0 \\ \frac{\sin\|\boldsymbol{\rho}\|}{\|\boldsymbol{\rho}\|}\boldsymbol{I}_3 - \frac{1-\cos\|\boldsymbol{\rho}\|}{\|\boldsymbol{\rho}\|^2}\widehat{\boldsymbol{\rho}}, & \boldsymbol{\rho} \neq \mathbf{0}' \end{cases} \tag{19}$$

where $\theta = \arccos\frac{\mathrm{trace}(R)-1}{2}$.

2) The *Cayley map* $\vartheta = \mathrm{cay}$ and its inverse $\vartheta^{-1} = \mathrm{cay}^{-1}$ are defined by:

$$\mathrm{cay}(\boldsymbol{\rho}) = \mathbf{I}_3 + \frac{4}{4 + \|\boldsymbol{\rho}\|^2}\left(\widehat{\boldsymbol{\rho}} + \frac{\widehat{\boldsymbol{\rho}}^2}{2}\right). \tag{20}$$

$$\mathrm{cay}^{-1}(R) = -2\left[(\boldsymbol{I}_3 + R)^{-1}(\boldsymbol{I}_3 - R)\right]^{\vee} \tag{21}$$

$$B_{\mathrm{cay}}(R) = \frac{4}{4 + \|\boldsymbol{\rho}\|^2}\left(\boldsymbol{I}_3 - \frac{\widehat{\boldsymbol{\rho}}}{2}\right). \tag{22}$$

3) Higher-order Rodriguez's parameters $\vartheta = \mathrm{rod}_2$ and $\vartheta^{-1} = \mathrm{rod}_2^{-1}$ (described in e.g. [33]).

The exponential and Cayley maps can represent rotation errors up to π radians. This range can be extended to 2π using the modified Rodriguez's parameters and to even larger ranges using higher-order Cayley mappings. In our implementation we employ $\vartheta = \mathrm{cay}$ since it has the simplest form, without any trigonometric functions or singularities at the origin.

B. Tracking errors

The control law is based on the error terms

$$\boldsymbol{e}_x = \boldsymbol{x} - \boldsymbol{x}_d, \qquad e_u = u - u_d,$$
$$\boldsymbol{e}_\omega = \boldsymbol{\omega} - R^T R_d \boldsymbol{\omega}_d, \qquad \boldsymbol{e}_R = \vartheta^{-1}(R_d^T R).$$

Additionally, define the modified terms $\widetilde{e}_{\dot{u}} \in \mathbb{R}$, $\widetilde{\boldsymbol{e}}_\omega \in \mathbb{R}^3$ by

$$\widetilde{e}_{\dot{u}} = \dot{e}_u + \frac{1}{k_u} \boldsymbol{e}^T R^T \dot{\boldsymbol{e}}_x, \tag{23}$$

$$\widetilde{\boldsymbol{e}}_\omega = \boldsymbol{e}_\omega + \frac{1}{k_R} \left(B_\vartheta \big(R_d^T R \big) \, \boldsymbol{e} u_d \right) \times R^T \dot{\boldsymbol{e}}_x. \tag{24}$$

These terms are key in obtaining a stable controller despite the non-trivial system underactuation.

C. Control Law

Proposition 2. *The control inputs $(u, \boldsymbol{\tau}, \boldsymbol{\tau}_r)$ given by*

$$\ddot{u} = -k_u e_u - k_{\dot{u}} \widetilde{e}_{\dot{u}} + \ddot{u}_d - \frac{1}{k_u} \left(\ddot{\boldsymbol{e}}_x^T R \boldsymbol{e} + \dot{\boldsymbol{e}}_x^T R (\boldsymbol{\omega} \times \boldsymbol{e}) \right),$$

$$\begin{bmatrix} \boldsymbol{\tau} \\ \boldsymbol{\tau}_r \end{bmatrix} = \begin{bmatrix} -k_R R^T R_d \boldsymbol{e}_R - k_\omega \widetilde{\boldsymbol{e}}_\omega - \boldsymbol{\mu} \times \boldsymbol{\omega} + C^T \boldsymbol{e} u/m \\ -k_r \boldsymbol{e}_r - k_{\dot{r}} \dot{\boldsymbol{e}}_r - \frac{1}{2} \overline{\boldsymbol{\xi}}^T \partial \overline{M}(\boldsymbol{r}) \overline{\boldsymbol{\xi}} + M_{v\dot{r}}^T \boldsymbol{e} u/m \end{bmatrix}$$
$$+ \dot{\boldsymbol{b}} + \frac{1}{2} \dot{\overline{M}}(\boldsymbol{r}) \begin{bmatrix} \widetilde{\boldsymbol{e}}_\omega \\ \dot{\boldsymbol{e}}_r \end{bmatrix},$$

where

$$\boldsymbol{b} = \overline{M}(\boldsymbol{r}) \begin{bmatrix} R^T R_d \left(\boldsymbol{\omega}_d - \frac{1}{k_R} B_\vartheta (R_d^T R) \boldsymbol{e} u_d \times R^T \dot{\boldsymbol{e}}_x \right) \\ \dot{\boldsymbol{r}}_d \end{bmatrix} \tag{25}$$

asymptotically track a given desired trajectory $(\boldsymbol{x}_d(t), R_d(t), \boldsymbol{r}_d(t))$.

Proof: see Appendix §C ■

D. Relation to other work.

Our approach for treating the error in rotation without resorting to coordinates such as Euler angles follows the development in [12]. For greater generality, we provide a general mapping with alternative choices for encoding this error. In particular, the Cayley map and its higher-order versions provide a simple alternative approach that leads to even further expansion of the region of asymptotic stability.

IV. Application: Hexrotor with a simple manipulator

The hexrotor shown in Figure 1 has three pairs of propellers fixed onto three spokes at 120 degrees. A two-link manipulator with a low-cost gripper is suspended from the vehicle and can extend forward between the two forward-facing spokes. Such an arrangement enables the manipulator tip to extend beyond the vehicle perimeter which enables interesting reaching maneuvers.

Ignoring the gripper motor, the manipulator has two degrees of freedom, i.e. $\boldsymbol{r} = (r_1, r_2)$. The forward kinematics are given by

$$g_{01}(\boldsymbol{r}) = \begin{pmatrix} c_1 & 0 & s_1 & -\frac{l_1}{2} s_1 \\ 0 & 1 & 0 & 0 \\ -s_1 & 0 & c_1 & -\frac{l_1}{2} c_1 \\ 0 & 0 & 0 & 1 \end{pmatrix}, \tag{26}$$

$$g_{02}(\boldsymbol{r}) = \begin{pmatrix} c_{12} & 0 & s_{12} & -\frac{l_2}{2} s_{12} - l_1 s_1 \\ 0 & 1 & 0 & 0 \\ -s_{12} & 0 & c_{12} & -\frac{l_2}{2} c_{12} - l_1 c_1 \\ 0 & 0 & 0 & 1 \end{pmatrix}, \tag{27}$$

$$g_{0t}(\boldsymbol{r}) = \begin{pmatrix} c_{12} & 0 & s_{12} & -l_2 s_{12} - l_1 s_1 \\ 0 & 1 & 0 & 0 \\ -s_{12} & 0 & c_{12} & -l_2 c_{12} - l_1 c_1 \\ 0 & 0 & 0 & 1 \end{pmatrix}, \tag{28}$$

using the shorthand notation $c_i := \cos r_i$, $s_i := \sin r_i$ for $i = 1, 2$ and $c_{12} := \cos(r_1 + r_2)$, $s_{12} := \sin(r_1 + r_2)$.

We assume that a desired trajectory is specified using a desired center of mass $\boldsymbol{x}_d(t) \in \mathbb{R}^3$ and manipulator tip position $\boldsymbol{y}_d(t) \in \mathbb{R}^3$. Let $I_x : SE(3) \to \mathbb{R}^3$ and $I_R : SE(3) \to SO(3)$ extract the position and orientation of a given pose. The required orientation R_d and joint angles $\boldsymbol{r}_d$ to track $\boldsymbol{y}_d$ are chosen to satisfy

$$\boldsymbol{y}_d = I_x \left(g_0(\boldsymbol{x}_d, R_d) g_{0t}(\boldsymbol{r}_d) \right). \tag{29}$$

The rotation R_d is chosen during closed-loop tracking so that $R_d \boldsymbol{e} = \boldsymbol{\alpha}$. This leaves an extra degree of freedom in R_d, i.e. rotating the frame around the $\boldsymbol{\alpha}$ axis. A desired $\boldsymbol{y}_d$ can be exactly achieved by setting

$$\boldsymbol{c}_3 = \frac{\alpha}{\|\alpha\|} \tag{30}$$

$$\boldsymbol{c}_2 = \frac{\boldsymbol{c}_3 \times (\boldsymbol{y}_d - \boldsymbol{x}_d)}{\|\boldsymbol{c}_3 \times (\boldsymbol{y}_d - \boldsymbol{x}_d)\|} \tag{31}$$

$$R_d = [\pm \boldsymbol{c}_2 \times \boldsymbol{c}_3 \mid \pm \boldsymbol{c}_2 \mid \boldsymbol{c}_3] \tag{32}$$

The required angles r_1, and r_2 are found through the relationship

$$I_x \left(g_{0t}(\boldsymbol{r}) \right) = R_d^T (\boldsymbol{y}_d - \boldsymbol{x}_d), \tag{33}$$

where only the first and third elements of the vectors on both sides are non-zero. The relation (33) is solved in closed form using standard inverse kinematics techniques. There are a total of four solutions $(R_d, \boldsymbol{r}_d)$ for any given $(\boldsymbol{x}_d, \boldsymbol{y}_d)$ since (30) gives two choices and (33) results in a quadratic equation with two roots.

Figures 2 and 3 show the simulated controller behavior during an aggressive reaching maneuver. The vehicle is required to track a path $(\boldsymbol{x}_d(t), \boldsymbol{y}_d(t))$ that extends the manipulator outside of the vehicle propeller range in order to reach a desired final point.

V. Conclusion

This paper studies trajectory tracking of articulated aerial systems. The developed controller employed existing results in free-flying multi-body system modeling, backstepping control of underactuated systems, and control on manifolds. The key

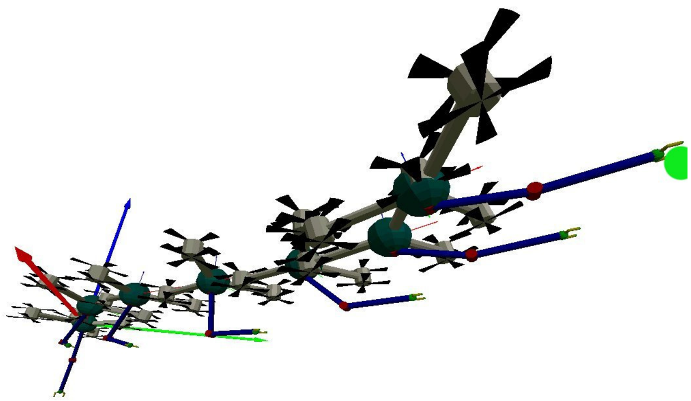

Fig. 2. Several frames along the simulated hexrotor trajectory reaching a desired point in workspace.

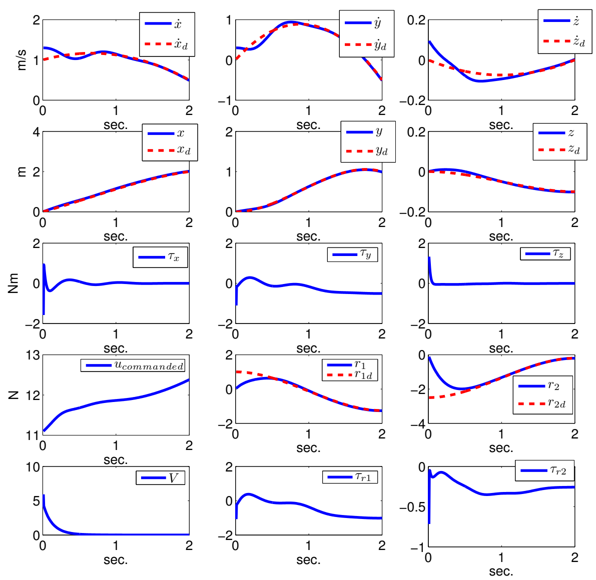

Fig. 3. History of the states, control inputs, and Lyapunov function V of the scenario shown in Fig. 2

contribution is to transform the system into a suitable form that enables dynamic extension and energy-based control, avoiding the use of rotational coordinates, proving stability for the coupled closed-loop system. Key issues that need to addressed is the sensitivity of the resulting controller to unmodeled disturbances in view of their effect on the higher-order derivatives present in the control law. Furthermore, bounds on the actuators need to be formally considered since aerial manipulation tasks would require inputs close to the vehicle operational envelope. Resolving these two issues is critical for rendering the proposed methods useful for practical applications.

Appendix

A. Dynamics of a free-floating multi-body vehicle

The variational principle used to obtain the dynamics is

$$\delta \int L_0(\boldsymbol{q}_0, \boldsymbol{\xi}_0)dt + \int \langle \boldsymbol{f}_0, \delta \boldsymbol{q}_0 \rangle = 0, \tag{34}$$

where $\boldsymbol{f}_0 = (R_0\boldsymbol{\tau}, R_0\boldsymbol{e}u, \boldsymbol{\tau}_r)$. The resulting equations of motion are obtained by taking variations $\delta\boldsymbol{\xi}_0 = (\delta\boldsymbol{\omega}_0, \delta\boldsymbol{v}_0, \delta\boldsymbol{r})$ and $\delta\boldsymbol{q}_0 = (\delta R_0, \delta\boldsymbol{x}_0, \delta\boldsymbol{r})$ which are constrained by $\delta\boldsymbol{\omega} = \dot{\boldsymbol{\eta}} + \boldsymbol{\omega}\times\boldsymbol{\eta}$ and $\delta\boldsymbol{v} = -\boldsymbol{\eta}\times\boldsymbol{v} + R^T\frac{d}{dt}\delta\boldsymbol{x}$, for $\boldsymbol{\eta} = (R^T\delta R)^{\check{}}$.

Using the momenta $\boldsymbol{\mu}_0 = \partial_{\boldsymbol{\omega}_0}L_0$, $\boldsymbol{p}_0 = \partial_{\boldsymbol{v}_0}L_0$ and $\boldsymbol{\nu} = \partial_{\dot{\boldsymbol{r}}}L$ the resulting dynamics can be expressed as:

$$\begin{bmatrix} \boldsymbol{\omega}_0 \\ \boldsymbol{v}_0 \\ \dot{\boldsymbol{r}} \end{bmatrix} = M_0(\boldsymbol{r})^{-1} \begin{bmatrix} \boldsymbol{\mu}_0 \\ \boldsymbol{p}_0 \\ \boldsymbol{\nu}_0 \end{bmatrix} \tag{35}$$

$$\begin{bmatrix} \dot{\boldsymbol{\mu}}_0 \\ \dot{\boldsymbol{p}}_0 \\ \dot{\boldsymbol{\nu}}_0 \end{bmatrix} = \begin{bmatrix} \boldsymbol{\mu}_0\times\boldsymbol{\omega}_0 + \boldsymbol{p}_0\times\boldsymbol{v}_0 \\ \boldsymbol{p}_0\times\boldsymbol{\omega}_0 \\ \frac{1}{2}{\boldsymbol{\xi}_0}^T\partial M_0(\boldsymbol{r})\boldsymbol{\xi}_0 \end{bmatrix} - \begin{bmatrix} R_0^T\partial_{R_0}V \\ R_0^T\partial_{\boldsymbol{x}_0}V \\ \partial_{\boldsymbol{r}}V \end{bmatrix} + \begin{bmatrix} \boldsymbol{\tau} \\ \boldsymbol{e}u \\ \boldsymbol{\tau}_r \end{bmatrix}. \tag{36}$$

The system evolution is then fully determined by adding the reconstruction equations $\dot{R}_0 = R_0\boldsymbol{\omega}_0$ and $\dot{\boldsymbol{x}}_0 = R_0\boldsymbol{v}_0$.

B. Proof of Proposition 1

It can be verified that a Lagrangian

$$L(\boldsymbol{q}, \boldsymbol{\xi}) = \frac{1}{2}m\boldsymbol{v}^T\boldsymbol{v} + \frac{1}{2}\bar{\boldsymbol{\xi}}^T\overline{M}(\boldsymbol{r})\bar{\boldsymbol{\xi}} - m\boldsymbol{a}_g^T\boldsymbol{x} \tag{37}$$

satisfies the relationship $L_0(\boldsymbol{q}_0, \boldsymbol{\xi}_0) = L(\boldsymbol{q}, \boldsymbol{\xi})$. The variational principle

$$\delta \int L(\boldsymbol{q}, \boldsymbol{\xi})dt + \int \langle \boldsymbol{f}, \delta\boldsymbol{q} \rangle dt = 0, \tag{38}$$

can then be used to obtain the dynamics, where

$$\begin{aligned}\langle \boldsymbol{f}, \delta\boldsymbol{q} \rangle =& \langle R\boldsymbol{e}u, \delta\boldsymbol{x} \rangle \\ &+ \langle \boldsymbol{\tau} - C^T\boldsymbol{e}u/m, R^T\delta R \rangle + \langle \boldsymbol{\tau}_r - M_{v\dot{r}}^T\boldsymbol{e}u/m, \delta r \rangle.\end{aligned}$$

The position dynamics is decoupled and results in the standard form (10). The relation (11) is the Legendre transform from momenta $\boldsymbol{\mu} = \partial_{\boldsymbol{\omega}}L$ and $\boldsymbol{\nu} = \partial_{\dot{\boldsymbol{r}}}L$ to velocities. The momenta evolution (12) is then derived by taking variations $(\delta R, \delta\boldsymbol{r})$ under the standard (e.g. [34]) rigid-body constraint $\delta\boldsymbol{\omega} = \dot{\boldsymbol{\eta}} + \boldsymbol{\omega}\times\boldsymbol{\eta}$ where $\boldsymbol{\eta} = (R^T\delta R)^{\check{}}$.

C. Proof of Proposition 2

Define the Lyapunov function

$$\begin{aligned} V =& \frac{k_x}{2}\|\boldsymbol{e}_x\|^2 + \frac{k_R}{2}\|\boldsymbol{e}_R\|^2 + \frac{k_r}{2}\|\boldsymbol{e}_r\|^2 + \frac{k_u}{2}e_u^2 \\ &+ \frac{m}{2}\|\dot{\boldsymbol{e}}_x\|^2 + \frac{1}{2}\begin{bmatrix} \tilde{\boldsymbol{e}}_\omega \\ \dot{\boldsymbol{e}}_r \end{bmatrix}^T \overline{M}(\boldsymbol{r}) \begin{bmatrix} \tilde{\boldsymbol{e}}_\omega \\ \dot{\boldsymbol{e}}_r \end{bmatrix} + \frac{1}{2}\tilde{e}_{\dot{u}}^2. \end{aligned} \tag{39}$$

Differentiating, and using the properties of the retraction map (e.g. [32])

$$\begin{aligned}\dot{V} =& k_x \boldsymbol{e}_x^T \dot{\boldsymbol{e}}_x + k_R \left[R^T R_d \boldsymbol{e}_R\right]^T \boldsymbol{e}_\omega + k_r \boldsymbol{e}_r^T \dot{\boldsymbol{e}}_r + k_u e_u \dot{e}_u \\ &+ m \dot{\boldsymbol{e}}_x^T (\ddot{\boldsymbol{x}} - \ddot{\boldsymbol{x}}_d) \\ &+ \left[\begin{array}{c} \widetilde{\boldsymbol{e}}_\omega \\ \dot{\boldsymbol{e}}_r \end{array}\right]^T \left(\left[\begin{array}{c} \dot{\boldsymbol{\mu}} \\ \dot{\boldsymbol{\nu}} \end{array}\right] - \dot{\boldsymbol{b}} - \frac{1}{2}\dot{\overline{M}}(\boldsymbol{r}) \left[\begin{array}{c} \widetilde{\boldsymbol{e}}_\omega \\ \dot{\boldsymbol{e}}_r \end{array}\right]\right) \\ &+ \widetilde{e}_{\dot{u}} \frac{d}{dt} \widetilde{e}_{\dot{u}}. \end{aligned} \tag{40}$$

Using the fact that

$$R^T \boldsymbol{\alpha} = R^T R_d \boldsymbol{e} u_d = \left[I - \widehat{\boldsymbol{e}_R} B_\vartheta (R_d^T R)\right] \boldsymbol{e} u_d,$$

we have

$$\begin{aligned}& k_k \boldsymbol{e}_x^T \dot{\boldsymbol{e}}_x + m \dot{\boldsymbol{e}}_x^T (\ddot{\boldsymbol{x}} - \ddot{\boldsymbol{x}}_d) = \\ &= -k_v \|\dot{\boldsymbol{e}}_x\|^2 + (R^T \dot{\boldsymbol{e}}_x)^T (\boldsymbol{e} u - R^T \boldsymbol{\alpha}) \\ &= -k_v \|\dot{\boldsymbol{e}}_x\|^2 + (R^T \dot{\boldsymbol{e}}_x)^T \left(e_u \boldsymbol{e} + \boldsymbol{e}_R \times B_\vartheta (R_d^T R) \boldsymbol{e} u_d\right), \end{aligned} \tag{41}$$

Then, after substituting (41) and the angular and joint dynamics (12)

$$\begin{aligned}\dot{V} =& - k_v \|\dot{\boldsymbol{e}}_x\|^2 + k_R \left[R^T R_d \boldsymbol{e}_R\right]^T \widetilde{\boldsymbol{e}}_\omega + k_r \boldsymbol{e}_r^T \dot{\boldsymbol{e}}_r + k_u e_u \dot{e}_u \\ &+ \begin{bmatrix} \widetilde{\boldsymbol{e}}_\omega \\ \dot{\boldsymbol{e}}_r \end{bmatrix}^T \left(\begin{bmatrix} \boldsymbol{\mu} \times \boldsymbol{\omega} + \boldsymbol{\tau} - C^T \boldsymbol{e} u/m \\ \frac{1}{2} \overline{\boldsymbol{\xi}}^T \partial \overline{M}(\boldsymbol{r}) \overline{\boldsymbol{\xi}} + \boldsymbol{\tau}_r - M_{v\dot{r}}^T \boldsymbol{e} u/m \end{bmatrix} \right. \\ &\qquad \left. - \dot{\boldsymbol{b}} - \frac{1}{2} \dot{\overline{M}}(\boldsymbol{r}) \begin{bmatrix} \widetilde{\boldsymbol{e}}_\omega \\ \dot{\boldsymbol{e}}_r \end{bmatrix} \right) \\ &+ \widetilde{e}_{\dot{u}} \left(\ddot{u} - \ddot{u}_d + \frac{d}{dt} \frac{1}{k_u} \dot{\boldsymbol{e}}_x^T R \boldsymbol{e} \right). \end{aligned} \tag{42}$$

Finally, after substituting the control $(\boldsymbol{\tau}, u, \boldsymbol{\tau}_r)$,

$$\dot{V} = - k_v \|\dot{\boldsymbol{e}}_x\|^2 - k_\omega \|\widetilde{\boldsymbol{e}}_\omega\|^2 - k_{\dot{r}} \|\dot{\boldsymbol{e}}_r\|^2 - k_{\dot{u}} (\widetilde{e}_{\dot{u}})^2. \tag{43}$$

Since $\dot{V} \leqslant 0$ with equality only when the extended error state is zero, by Barbalat's lemma the system is asymptotically stable.

References

[1] P. Pounds, D. Bersak, and A. Dollar, "The yale aerial manipulator: Grasping in flight," in *Robotics and Automation (ICRA), 2011 IEEE International Conference on*, may 2011, pp. 2974 –2975.

[2] P. E. I. Pounds, D. R. Bersak, and A. M. Dollar, "Stability of small-scale uav helicopters and quadrotors with added payload mass under pid control," *Auton. Robots*, vol. 33, no. 1-2, pp. 129–142, 2012.

[3] Q. J. Lindsey, D. Mellinger, and V. Kumar, "Construction of cubic structures with quadrotor teams," *Robotics: Science and Systems*, June 2011.

[4] M. Hehn and R. D'Andrea, "A flying inverted pendulum," in *Robotics and Automation (ICRA), 2011 IEEE International Conference on*, may 2011, pp. 763 –770.

[5] C. M. Korpela, T. W. Danko, and P. Y. Oh, "Mm-uav: Mobile manipulating unmanned aerial vehicle," *J. Intell. Robotics Syst.*, vol. 65, no. 1-4, pp. 93–101, Jan. 2012. [Online]. Available: http://dx.doi.org/10.1007/s10846-011-9591-3

[6] C. Korpela, M. Orsag, T. Danko, B. Kobe, C. McNeil, R. Pisch, and P. Oh, "Flight stability in aerial redundant manipulators," in *Robotics and Automation (ICRA), 2012 IEEE International Conference on*, may 2012, pp. 3529 –3530.

[7] C. Korpela, T. Danko, and P. Oh, "Designing a system for mobile manipulation from an unmanned aerial vehicle," in *Technologies for Practical Robot Applications (TePRA), 2011 IEEE Conference on*, april 2011, pp. 109 –114.

[8] Airobots, "http://airobots.ing.unibo.it."

[9] ARCAS, "http://www.arcas-project.eu."

[10] D. Fusata, G. Guglieri, and R. Celi, "Flight dynamics of an articulated rotor helicopter with an external slung load," *Journal of the American Helicopter Society*, vol. 46, no. 1, pp. 3–14, 2001.

[11] T. Koo and S. Sastry, "Output tracking control design of a helicopter model based on approximate linearization," in *Decision and Control, 1998. Proceedings of the 37th IEEE Conference on*, vol. 4, dec 1998, pp. 3635 –3640 vol.4.

[12] E. Frazzoli, M. Dahleh, and E. Feron, "Trajectory tracking control design for autonomous helicopters using a backstepping algorithm," in *American Control Conference, 2000. Proceedings of the 2000*, vol. 6, 2000, pp. 4102–4107.

[13] R. Mahony and T. Hamel, "Robust trajectory tracking for a scale model autonomous helicopter," *International Journal of Robust and Nonlinear Control*, vol. 14, no. 12, pp. 1035–1059, 2004. [Online]. Available: http://dx.doi.org/10.1002/rnc.931

[14] S. Dubowsky and E. Papadopoulos, "The kinematics, dynamics, and control of free-flying and free-floating space robotic systems," *Robotics and Automation, IEEE Transactions on*, vol. 9, no. 5, pp. 531 –543, oct 1993.

[15] R. Mukherjee and D. Chen, "Control of free-flying underactuated space manipulators to equilibrium manifolds," *Robotics and Automation, IEEE Transactions on*, vol. 9, no. 5, pp. 561 –570, oct 1993.

[16] A. Jain, *Robot and Multibody Dynamics: Analysis and Algorithms*. Springer, 2011.

[17] M. W. Spong, "Underactuated mechanical systems," in *Control Problems in Robotics and Automation*. Springer-Verlag, 1998.

[18] J. Descusse and C. H. Moog, "Dynamic decoupling for right-invertible nonlinear systems," *Syst. Control Lett.*, vol. 8, no. 4, pp. 345–349, Mar. 1987. [Online]. Available: http://dx.doi.org/10.1016/0167-6911(87)90101-0

[19] J. Hauser, S. Sastry, and G. Meyer, "Nonlinear control design for slightly non-minimum phase systems: Application to v/stol aircraft," *Automatica*, vol. 28, no. 4,

pp. 665 – 679, 1992. [Online]. Available: http://www.sciencedirect.com/science/article/pii/000510989290029F

[20] E. Altug, J. P. Ostrowski, and R. E. Mahony, "Control of a quadrotor helicopter using visual feedback," in *International Conference on Robotics and Automation*, 2002, pp. 72–77.

[21] S. Al-Hiddabi, "Quadrotor control using feedback linearization with dynamic extension," in *Mechatronics and its Applications, 2009. ISMA '09. 6th International Symposium on*, march 2009, pp. 1 –3.

[22] D. Lee, H. Jin Kim, and S. Sastry, "Feedback linearization vs. adaptive sliding mode control for a quadrotor helicopter," *International Journal of Control, Automation and Systems*, vol. 7, pp. 419–428, 2009, 10.1007/s12555-009-0311-8. [Online]. Available: http://dx.doi.org/10.1007/s12555-009-0311-8

[23] S. Bouabdallah and R. Siegwart, "Backstepping and sliding-mode techniques applied to an indoor micro quadrotor," in *Robotics and Automation, 2005. ICRA 2005. Proceedings of the 2005 IEEE International Conference on*, april 2005, pp. 2247 – 2252.

[24] T. Madani and A. Benallegue, "Control of a quadrotor mini-helicopter via full state backstepping technique," in *Decision and Control, 2006 45th IEEE Conference on*, dec. 2006, pp. 1515 –1520.

[25] P. Adigbli, C. Grand, J. baptiste Mouret, and S. Doncieux, "Nonlinear attitude and position control of a micro quadrotor using sliding mode and backstepping techniques," in *European Micro Air Vehicle Conference and Flight Competition (EMAV2007)*, 2007.

[26] G. Raffo, M. Ortega, and F. Rubio, "Backstepping/nonlinear h-infty control for path tracking of a quadrotor unmanned aerial vehicle," in *American Control Conference, 2008*, june 2008, pp. 3356 –3361.

[27] J. Colorado, A. Barrientos, A. Martinez, B. Lafaverges, and J. Valente, "Mini-quadrotor attitude control based on hybrid backstepping amp; frenet-serret theory," in *Robotics and Automation (ICRA), 2010 IEEE International Conference on*, may 2010, pp. 1617 –1622.

[28] I.-H. Choi and H.-C. Bang, "Adaptive command filtered backstepping tracking controller design for quadrotor unmanned aerial vehicle," *Proceedings of the Institution of Mechanical Engineers, Part G: Journal of Aerospace Engineering*, vol. 226, no. 5, pp. 483–497, 2012. [Online]. Available: http://pig.sagepub.com/content/226/5/483.abstract

[29] R. Olfati-Saber, "Nonlinear control of underactuated mechanical systems with application to robotics and aerospace vehicles," Ph.D. dissertation, Massachusetts Institute of Technology, 2001, aAI0803036.

[30] T. Lee, M. Leok, and N. McClamroch, "Geometric tracking control of a quadrotor uav on se(3)," in *Decision and Control (CDC), 2010 49th IEEE Conference on*, dec. 2010, pp. 5420 –5425.

[31] R. M. Murray, Z. Li, and S. S. Sastry, *A Mathematical Introduction to Robotic Manipulation*. CRC, 1994.

[32] F. Bullo and A. Lewis, *Geometric Control of Mechanical Systems*. Springer, 2004.

[33] P. Tsiotras, "Higher order cayley transforms with applications to attitude representations," *Journal of Guidance, Control, and Dynamics*, vol. 20, 1997.

[34] J. E. Marsden and T. S. Ratiu, *Introduction to Mechanics and Symmetry*. Springer, 1999.